Med Chem Res (2010) 19:103–119
DOI 10.1007/s00044-009-9175-y

MEDICINAL CHEMISTRY RESEARCH

ORIGINAL RESEARCH

Design, synthesis, and structure–activity relationship study of 5-amido-1-(2,4-dinitrophenyl)-1*H*-4-pyrazolecarbonitrils as DD-carboxypeptidase/penicillin-binding protein inhibitors with Gram-positive antibacterial activity

Hamid Sadeghian · Ali Sadeghian · Mehdi Pordel · Mohammad Rahimizadeh · Pooneh Jahandari · Ala Orafaie · Mehdi Bakavoli

Received: 20 September 2008 / Accepted: 10 February 2009 / Published online: 8 April 2009

Abstract In this study, we report the design, synthesis, and structure–activity relationships of a series of 5-amido-1-(2,4-dinitrophenyl)-1*H*-4-pyrazolecarbonitriles as DD-carboxypeptidase/penicillin-binding protein (PBP) inhibitors with Gram-positive antibacterial activity. Our results show that the compounds with larger, more polarizable, and electron-rich substituted benzamide moieties such as *para*-dimethyaminobenzamide (**3j**) and *para*-methoxybenzamide (**3i**) exhibit better antibacterial activity against methicillin-susceptible *Staphylococcus aureus* and methicillin-resistant *Staphylococcus aureus* with minimum inhibition concentration (MIC) values of 3.8 and 15.3 μM for both of them. These results are in accordance

H. Sadeghian
School of Paramedical Sciences, Mashhad University of Medical Sciences, Mashhad, Islamic Republic of Iran

A. Sadeghian (✉)
Microbiology and Virology Research Center, Buali Research Institute, Mashhad University of Medical Sciences, Mashhad 9196773117, Islamic Republic of Iran
e-mail: Sadeghiana@mums.ac.ir

M. Pordel · P. Jahandari · M. Bakavoli
Department of Chemistry, School of Sciences, Ferdowsi University of Mashhad, Mashhad, Islamic Republic of Iran

M. Rahimizadeh
Department of Chemistry, Faculty of Sciences, Ferdowsi University of Mashhad, Mashhad, Islamic Republic of Iran

A. Orafaie
Department of Biology, School of Sciences, Ferdowsi University of Mashhad, Mashhad, Islamic Republic of Iran

with estimated inhibition constants (K_i) that are obtained from docking with PBP2 and PBP4 of *Staphylococcus aureus*.

Keywords *Staphylococcus aureus* · Docking · MIC · Multiple alignment · β-Lactamase

Introduction

In recent years, antimicrobial resistance has become a global issue of great importance in many countries around the world (Cookson, 2005). The contribution of pyrazole derivatives in prevention of bacterial infections (Patel *et al.*, 1990) directed us to search for new antimicrobial compounds.

Heterocyclic pyrazoles, containing phenyl and nitrophenyl substituent on nitrogen atom, are known to posses antibacterial activities (Ammar *et al.*, 2004; Ergenc *et al.*, 1992; Schmidt *et al.*, 1958). The clinical significance of this class of compounds has stimulated the synthesis of new lead compounds retaining the core pyrazole chromophore. To find new substituted pyrazoles with antibacterial activity, we have designed and synthesized a series of 5-amino-1-(2,4-dinitrophenyl)-1*H*-4-pyrazolecarbonitrile carboxylate **3a–j** (Fig. 1). The amide group is essential to exhibit antibacterial activities. These compounds were only effective against Gram-positive bacteria. Structure–activity relationships (SAR) have been employed from the start and throughout the study to correlate information in data sets and lead the study to the right direction to find more active compounds. For proposing key futures of this class of inhibitors the antibacterial effects of the compounds were studied on *S. aureus*, as a representative of Gram-positive bacteria. The results of evaluation (MIC) were then compared with SAR calculations. A large number of such SAR models have been developed for different biological properties (Ghafourian and Barzegar-Jalali 2002; Free and Wilson, 1964; Ghafourian and Hansch, 2003; Nieto *et al.*, 2005). Recently, we reported the development of useful SAR models for antibacterial (Sadeghian *et al.*, 2007) and 15-lipoxygenase inhibitory activities (Bakavoli *et al.*, 2007, 2008; Sadeghian *et al.*, 2008).

Following our previous work on 5-amino-1-(2,4-dinitrophenyl)-1*H*-4-pyrazolecarbonitrile **1** and 5-acetamido-1-(2,4-dinitrophenyl)-1*H*-4-pyrazolecarbonitrile **3a**[1] (Pordel, 2004) we tested the inhibitory property of **3a–d** against two Gram-negative strains of bacteria, *Pseudomanas aeruginosa* and *Klebsiella pneumoniae*, and a Gram-positive bacteria *Staphylococcuse aureus*. Compounds **3a–d** exhibited moderate to weak antibacterial activities only against *S. aureus* pathogen (MIC = 316.0, 195.4, 57.4, and 132.3 μM, respectively). Compound **3c** was effective against the Gram-negative strains at higher concentration (MIC > 300 μM). Compounds **3a**, **b**, and **d** were not effective against the Gram-negative types, even at concentrations

[1] In this study the MIC values of compound **1** and **3a** against three Gram-negative (*Escherichia coli*, *Pseudomonas aeruginosa*, and *Klebsiella pneumonia*) and three Gram-positive (*Streptococcus pyrogenes*, *Streptococcus pneumonia*, and *Staphylococcus aureus*) strains of bacteria were determined. Among them only Gram-positive types were affected by compound **3a** (MIC = 100–400 μg/mL). None of the bacteria were affected by compound **1**.

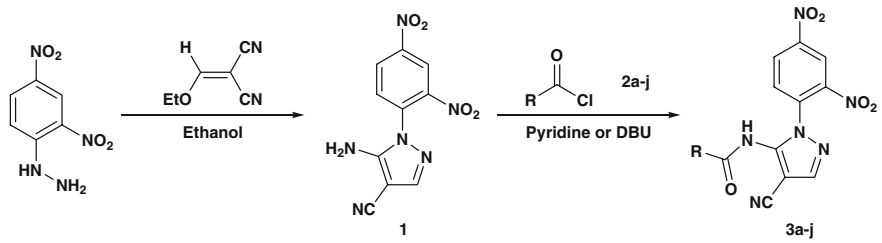

R	Compd.	MRSA	MSSA	R	Compd.	MRSA	MSSA
-CH_3	3a	632.0	316.0	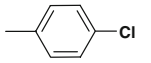	3f	60.5	60.5
	3b	390.8	195.4	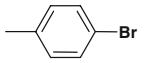	3g	27.4	27.4
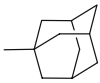	3c	57.4	57.4	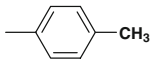	3h	63.8	31.9
	3d	264.5	132.3	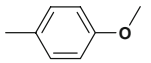	3i	15.3	15.3
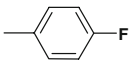	3e	252.5	126.3	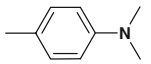	3j	3.8	3.8
Cephalexin		72.0	4.6	Cloxacillin		94.0	13.7

Fig. 1 General procedure for the synthesis of compounds **3a–j** (*above*) and the MIC values of compounds **3a–j** and two β-lactam antibiotics (cephalexin and cloxacillin) against two selected strains of *Staphylococcus aureus* (units of μM)

above 1,000 μM. On the basis of the selective antimicrobial effect of compounds **3a–d** against Gram-positive bacteria and the previously published data on the inhibitory activity of some pyrazole derivatives against bacterial cell wall biosynthesis (Li *et al.*, 2003), one can assumed that the bactericide effect is closely related to the inhibition of cell wall formation.

Normally the thick, homogeneous cell wall of Gram-positive bacteria is composed of multilayered peptidoglycan polymer, which often contains a peptide interbridge, while comparatively Gram-negative cell walls are much more complex and contain outer membrane, periplasmic space, and peptidoglycan. The thin peptidoglycan layer next to the plasma membrane constitutes not more than 5–10% of the cell wall weight (Prescott *et al.*, 2002). Peptidoglycan biosynthesis requires more than ten synthetic transformations, each of which requires a specific enzyme (Bugg and Walsh 1992). These enzymes include MurA, MurB, MurC, MurD, MurE, MurF, MraY, MurG, and the transglycosylase and transpeptidase families of enzymes.

By taking into account the difference between activity of compound **1** (none effective) and its amide derivatives against Gram-positive bacteria and the

inhibitory nature of some non-β-lactam amides against β-lactamases and DD-peptidases (Adediran *et al.*, 2006; Ahn and Pratt, 2004; Pratt and Govardhan, 1984), it can be argued that, among the cell wall biosynthetic enzymes, the peptidoglycan cross-linking transpeptidase is the probable candidate for interference in bacterial growth. This enzyme is capable of cleaving the peptidoglycan D-Ala-D-Ala terminus in the serine acylation half reaction. To support this hypothesis several amides **3a–j** (Fig. 1) were designed, synthesized, and screened against *Staphylococcuse aureus* pathogens (methicillin-resistant *S. aureus* (MRSA) and methicillin-susceptible *S. aureus* (MSSA–ATCC 1112). Then complimentary SAR studies were carried out to evaluate the common bonding model of the synthetic amides in PBP active site and eventually propose key features of this class of compounds.

Materials and methods

Experimental

Melting points were recorded on an Electrothermal type 9100 melting point apparatus. The ^{1}H nuclear magnetic resonance (NMR) (100 MHz) spectra were recorded on a Bruker AC 100 spectrometer. Elemental analysis was obtained on a Thermo Finnigan Flash EA microanalyzer. Measurement of β-lactamase activity was carried out using an Agilent 8453 spectrophotometer. All of the chemicals were purchased from Sigma, Fluka, Calbiochem, and Merck Co. The microorganisms *S. aureus* ATCC 1112 was purchased from Pasteur Institute of Iran and *S. aureus* (methicillin resistant) was isolated from different specimens that were referred to the Microbiological Laboratory of Ghaem Hospital of Medical University of Mashhad, Iran, and its methicillin resistance was tested according to the NCCLS guidelines (Finegold and Garrod, 1995).

General procedure for preparation of the 5-amido-1-(2,4-dinitrophenyl)-1H-4-pyrazolecarbonitrile (**3a–j**)

A mixture of ethoxymethylenmalononitril (12.2 g, 100 mmol) and 2,4-dinitrophenylhydrazine (19.8 g, 100 mmol) in ethanol (200 mL) was heated under reflux for 4 h. After cooling, crystals of product were appeared. Then the crystals were separated and washed with ethanol and dried at 70°C to give **1** (18.4 g, 67%, mp 218°C).

To a stirred solution of **1** (2.74 g, 10 mmol) in dry pyridine (20 mL) was added acid chlorides **2a–i** (12 mmol) dropwise at room temperature. The mixture was stirred for 4 h at room temperature. After reaction completion, pyridine was evaporated under reduced pressure. The residue was treated with 5% sodium carbonate (2 × 50 mL) and extracted with dichloromethane (2 × 30 mL). The organic extract was dried with anhydrous sodium sulfate, concentrated under reduced pressure, and crystallized to provide the pure desired compound **3a–j**.

For preparation of compound **3j**, the hydrochloride salt of 4-(dimethylamino)benzoyl chloride **2j** (2.43 g, 12 mmol) was added to a solution of (2.74 g, 10 mol) of **1** and 1.7 g DBU in 50 ml chloroform while stirring in ice-water. After removing

from the ice-bath, the reaction mixture was stirred at room temperature for 12 h. The resulting solution was washed with 5% HCl (2 × 50 mL), 5% sodium carbonate (2 × 50 mL), and water (2 × 50 mL). The nonaqueous layer was dried over sodium sulfate. After removing of the solvent under reduced pressure, the residue was recrystallized to give **3j**.

5-Acetamido-1-(2,4-dinitrophenyl)-1*H*-4-pyrazolecarbonitrile (**3a**)

Light yellow crystals (methanol). Yield: 69%; mp 298°C. IR: 1705 (C=O) and 3217 (NH) cm^{-1}. ^1H NMR ($CDCl_3$): δ 1.99 (s, 3H), 8.08 (d, 1H, $J = 8.9$ Hz), 8.37 (s, 1H), 8.70 (d, 1H, $J = 8.9$ Hz), 8.94 (s, 1H), 10.99 (broad, 1H); Found: C, 45.39; H, 2.61; N, 26.49. $C_{12}H_8N_6O_5$ requires: C, 45.58; H, 2.55; N, 26.58%.

5-Cyclohexamido-1-(2,4-dinitrophenyl)-1*H*-4-pyrazolecarbonitrile (**3b**)

Light yellow crystals (dichloromethane/*n*-hexane). Yield: 78%; mp 107°C. IR: 1705 (C=O) and 3231 (NH) cm^{-1}. ^1H NMR ($CDCl_3$): δ 1.10-2.32 (m, 10H), 2.43 (m, 1H), 7.73 (br, 1H), 7.90 (d, 1H, $J = 8.0$ Hz), 8.01 (s, 1H), 8.61 (d, 1H, $J = 8.0$ Hz), 8.90 (s, 1H); Found: C, 53.22; H, 4.15; N, 21.74. $C_{17}H_{16}N_6O_5$ requires: C, 53.12; H, 4.20; N, 21.87%.

5-Adamantamido-1-(2,4-dinitrophenyl)-1*H*-4-pyrazolecarbonitrile (**3c**)

Light yellow crystals (dichloromethane/*n*-hexane). Yield: 73%; mp 212°C. IR: 1653 (C=O) and 3230 (NH) cm^{-1}. ^1H NMR ($CDCl_3$): δ 1.76 (m, 9H), 2.07 (m, 6H), 7.68 (broad, 1H), 7.95 (d, 1H, $J = 8.9$ Hz), 8.03 (s, 1H), 8.62 (d, 1H, $J = 8.9$ Hz), 8.88 (s, 1H); Found: C, 57.74; H, 4.65; N, 19.25. $C_{21}H_{20}N_6O_5$ requires: C, 57.79; H, 4.62; N, 19.26%.

5-Benzamido-1-(2,4-dinitrophenyl)-1*H*-4-pyrazolecarbonitrile (**3d**)

Light yellow crystals (dichloromethane/*n*-hexane). Yield: 81%; mp 133°C. IR: 1704 (C=O) and 3228 (NH) cm^{-1}. ^1H NMR ($CDCl_3$): δ 7.38–7.80 (m, 5H), 8.02 (d, 1H, $J = 6.4$ Hz), 8.07 (s, 1H), 8.50 (broad, 1H), 8.62 (d, 1H, $J = 6.4$ Hz), 8.80 (s, 1H); Found: C, 53.92; H, 2.68; N, 22.09. $C_{17}H_{10}N_6O_5$ requires: C, 53.97; H, 2.66; N, 22.22%.

5-(4-Flurobenzamido)-1-(2,4-dinitrophenyl)-1*H*-4-pyrazolecarbonitrile (**3d**)

Light yellow crystals (methanol). Yield: 67%; mp 127°C. IR: 1704 (C=O) and 3232 (NH) cm^{-1}. ^1H NMR ($CDCl_3$): δ 7.08–7.25 (m, 2H), 7.68–7.85 (m, 2H), 8.08 (d, 1H, $J = 6.4$ Hz), 8.12 (s, 1H), 8.38 (broad, 1H), 8.62 (d, 1H, $J = 6.4$ Hz), 8.84 (s, 1H); Found: C, 52.63; H, 2.25; N, 21.25. $C_{17}H_9FN_6O_5$ requires: C, 51.52; H, 2.29; N, 21.21%.

5-(4-Chlorobenzamido)-1-(2,4-dinitrophenyl)-1*H*-4-pyrazolecarbonitrile (**3d**)

Light yellow crystal (methanol). Yield: 63%; mp 126°C. 1705 (C=O) and 3230 (NH) cm^{-1}. ^1H NMR ($CDCl_3$): δ 7.48 (d, 2H, $J = 8.4$), 7.73 (d, 2H, $J = 8.4$), 8.05

(d, 1H, $J = 6.4$ Hz), 8.15 (s, 1H), 8.65 (d, 1H, $J = 6.4$ Hz), 8.69 (broad, 1H), 8.85 (s, 1H); Found: C, 49.39; H, 2.23; N, 19.31. $C_{17}H_9ClN_6O_5$ requires: C, 49.47; H, 2.20; N, 19.38%.

5-(4-Bromobenzamido)-1-(2,4-dinitrophenyl)-1*H*-4-pyrazolecarbonitrile (**3d**)

Light yellow crystals (dichloromethane/*n*-hexane). Yield: 66%; mp 141°C. IR: 1705 (C=O) and 3243 (NH) cm^{-1}. ^1H NMR ($CDCl_3$): δ 7.75 (d, 2H, $J = 8.3$), 7.87 (d, 2H, $J = 8.3$), 8.18 (d, 1H, $J = 6.4$ Hz), 8.31 (s, 1H), 8.77 (d, 1H, $J = 6.4$ Hz), 8.92 (s, 1H), 10.57 (broad, 1H); Found: C, 44.53; H, 1.97; N, 18.26. $C_{17}H_9BrN_6O_5$ requires: C, 44.66; H, 1.98; N, 18.38%.

5-(4-Methylbenzamido)-1-(2,4-dinitrophenyl)-1*H*-4-pyrazolecarbonitrile (**3d**)

Light yellow crystals (chloroform/ethanol). Yield: 71%; mp 124°C. IR: 1679 (C=O) and 3241 (NH) cm^{-1}. ^1H NMR ($CDCl_3$): δ 2.38 (s, 3H), 7.35 (d, 2H, $J = 8.3$), 7.83 (d, 2H, $J = 8.3$), 8.22 (d, 1H, $J = 6.4$ Hz), 8.28 (s, 1H), 8.75 (d, 1H, $J = 6.4$ Hz), 8.89 (s, 1H), 10.35 (broad, 1H); Found: C, 55.12; H, 3.11; N, 21.40. $C_{18}H_{12}N_6O_5$ requires: C, 55.11; H, 3.08; N, 21.42%.

5-(4-Methoxybenzamido)-1-(2,4-dinitrophenyl)-1*H*-4-pyrazolecarbonitrile (**3d**)

Light yellow crystals (chloroform/ethanol). Yield: 49%; mp 98°C. IR: 1667 (C=O) and 3244 (NH) cm^{-1}. ^1H NMR ($CDCl_3$): δ 3.84 (s, 3H), 6.95 (d, 2H, $J = 8.5$), 7.65 (d, 2H, $J = 8.5$), 8.00 (d, 1H, $J = 6.4$ Hz), 8.04 (s, 1H), 8.45 (broad, 1H), 8.60 (d, 1H, $J = 6.4$ Hz), 8.75 (s, 1H); Found: C, 53.09; H, 2.95; N, 20.49. $C_{18}H_{12}N_6O_6$ requires: C, 52.95; H, 2.96; N, 20.58%.

5-(4-Dimethylaminobenzamido)-1-(2,4-dinitrophenyl)-1*H*-4-pyrazolecarbonitrile (**3d**)

Light brown crystals (dichloromethane/*n*-hexane). Yield: 32%; mp 112°C. IR: 1647 (C=O) and 3230 (NH) cm^{-1}. ^1H NMR ($CDCl_3$): δ 2.46 (s, 6H), 6.97 (d, 2H, $J = 8.5$), 8.07 (d, 2H, $J = 8.5$), 8.24 (d, 1H, $J = 6.4$ Hz), 8.26 (s, 1H), 8.73 (d, 1H, $J = 6.4$ Hz), 8.86 (s, 1H), 10.13 (broad, 1H); Found: C, 53.95; H, 3.66; N, 23.39. $C_{19}H_{15}N_7O_5$ requires: C, 54.16; H, 3.59; N, 23.27%.

Chemistry

The novel 5-amino-1-(2,4-dinitrophenyl)-1*H*-4-pyrazolecarbonitrile carboxylates **3a–j** (Fig. 1), were obtained from the precursor 5-amino-1-(2,4-dinitrophenyl)-1*H*-4-pyrazolecarbonitrile **1** and corresponding acid chlorides **2a–j**, which were either purchased or prepared (**3c** and **j**) by reaction of thionyl chloride and corresponding carboxylic acids (Villani and King, 1963). All desired amides (except **3j**) were synthesized by the action of the acid chlorides with compound **1** in dry pyridine.

Compound **3j** was prepared from the acid chloride **2j** with reagent **1** in the presence of 1,8-diazabicyclo[5.4.0]undec-7-ene (DBU) in chloroform. Compound **1** was synthesized according to literature (Kreutzberger and Burgwitz, 1980) by the action of 2,4-dinitrophenyl hydrazine with ethoxymethylenmalononitril in ethanol under reflux conditions.

Structural assignments of compounds **3a–j** was based upon spectral and microanalytical (C, H and N) data.

Bioinformatics, molecular modeling, docking, and QSAR study

Structure optimization

Structures **3a–j** were simulated by using chem3D professional Cambridge software, using MM2 method (RMS gradient = 0.05 kcal/mol) (ChemDraw 8.0, CambridgeSoft Corporation, http://www.cambrigesoft.com). Output files were minimized under semi-empirical AM1 method in the second optimization (convergence limit = 0.01; iteration limit = 50; RMS gradient = 0.05 kcal/mol; Fletcher–Reeves optimizer algorithm) in HyperChem7.5 (HyperChem 7.0, Hypercube Inc., http://www.hyper.com) (Bakavoli *et al.*, 2007).

Crystal structures of *Staphylococcus aureus* penicillin binding protein 2 and 4 (SPBP2 and SPBP4) were retrieved from RCSB Protein Data Bank (PDB entry: 2OLV and 1TVF, respectively).

Multiple alignment

Highly conserved amino acids were identified through multiple alignments on clustalX 1.81 (Thompson *et al.*, 1997) software. Sequences of penicillin binding proteins (PBP) family were selected from blasted sequences *via* ExPASY proteomics server (http://us.expasy.org/) with *E*-value < 0.02. Multiple alignment process was then carried out on the selected sequences (protein weight matrix: BLOSUM series, gap penalty = 10%).

Molecular docking

Automated docking simulation was implemented to dock **3a–j** into the active sites of SPBP2 and SPBP4 with AutoDock version 1.4 (Auto Dock Tools (ADT), http://www.scripps.edu/pub/olson-web/doc/autodock/) (Python, 1999) using Lamarckian genetic algorithm. This method has been previously shown to produce bonding modes similar to the experimentally observed modes (Dym *et al.*, 2002; Morris *et al.*, 1998; Sadeghian *et al.*, 2008). The torsion angles of the ligands were identified, hydrogens were added to the macromolecule, bond distances were edited, and solvent parameters were added to the enzyme three-dimensional (3D) structure. Partial atomic charges were then assigned to the macromolecule as well as ligands (Gasteiger for the ligands and Kollman for the protein).

Table 1 Data obtained from docking and QSAR analyses. (ΔG_b, estimated free energy of bonding; E_d, final docking energy; K_i, estimated inhibition constant

Compound	SPBP2			SPBP4		
	K_i	ΔG_b	E_d	K_i	ΔG_b	E_d
3a	144e−7	−6.61	−9.37	389e−9	−8.74	−11.01
3b	4.40e−7	−8.72	−9.06	7.31e−9	−11.10	−11.33
3c	5.79e−7	−8.51	−11.06	37.6e−9	−11.13	−12.28
3d	31.1e−7	−7.51	−8.24	16.9e−9	−10.60	−10.95
3e	26.3e−7	−7.58	−10.19	17.5e−9	−10.58	−13.31
3f	6.95e−7	−8.40	−11.36	7.08e−9	−11.12	−13.43
3g	3.10e−7	−8.90	−11.50	7.39e−9	−11.09	−13.61
3h	6.99e−7	−8.40	−11.12	6.44e−9	−11.17	−13.66
3i	5.03e−7	−8.59	−10.97	5.43e−9	−11.28	−13.82
3j	1.85e−7	−9.19	−11.51	2.27e−9	−11.79	−14.51

The unit of ΔG_b and E_d data is kcal/mol

The regions of interest of the enzyme were defined by considering Cartesian chart as –14.8, 20.6, and –10.0 for SPBP2 and 18.5, –2.0, and 20.4 for SPBP4 as the centrals of grid size of 50, 50, and 50 points in the *X*, *Y*, and *Z*-axes. The docking parameter files were generated using genetic algorithm and local search (GALS) parameters while number of generations was set to 100. Compound **3a–j** were each docked into the active sites of SPBP enzymes and the simulations were composed of 100 docking runs, each of 50 cycles containing a maximum of 10,000 accepted and rejected steps. The simulated annealing procedure was started at high temperature ($RT = 616$ kcal/mol, where R is the gas constant and T is the steady-state temperature) and was decreased by a fraction of 0.95 on each cycle (Sippl, 2000). The 100 docked complexes were clustered with a root-mean-square deviation tolerance of 0.1 Å. The program generated 100 docked conformers of **3a–j** corresponding to the lowest-energy structures. After docking procedure in AD3, docking results were submitted to Weblab Viewerlite 4.0 (http://sunfire.vbi.vt.edu/gcg/seqweb-guides/WebLab_Viewer.html) and Swiss-PdbViewer 3.7 (spdbv) (http://www.expasy.org/spdbv/) for further evaluations. The results of docking processing (ΔG_b, the estimated free energy of bonding; E_d, the final docked energy; K_i, the estimated inhibition constant) are outlined in Table 1.

Biological evaluations

Determination of MICs

The MICs of **3a–j** were determined by dilution tube test method, introduced by National Committee for Clinical Laboratory Standards (NCCLS) (Finegold and Garrod, 1995). For broth dilution methods, in which decreasing concentrations of the antimicrobial agents must be tested, usually serial twofold dilution of broth medium is placed in tubes which will support the growth of the test microorganism

[10^4 colony-forming units (CFU)/mL]. After sufficient incubation (18 h), the tubes are examined for turbidity, indicating growth of the microorganism. The organism will grow in tubes that do not contain enough antimicrobial agents to inhibit growth. For further confidence, the samples were cultured onto Petri dishes containing Muller–Hinton agar (18 h at 37°C). The lowest drug concentration of the agent that prevented growth of the test organism, as detected by lack of visual turbidity (matching the negative growth control), was designated the minimum inhibitory concentration (MIC). A serial dilution of tested compounds (final concentration of 400 to 0.4 μg/mL), were added to the test bacteria in Mueller–Hinton broth and were incubated at 37°C for 18 h. Growth was present in the medium control and was absent from the inoculum control (Phillips *et al.*, 1978).

Preparation of β-lactamase

Cells (methicillin-resistant *Staphylococcus aureus*) from the exponential growth phase were harvested by centrifugation for 10 min at 5,000 × g, washed once, and suspended in 0.1 M phosphate buffer (pH 7.0). The cell suspensions were sonicated at 20 kHz for 10 min. After the cellular debris was removed by centrifugation, the supernatant was used for testing of β-lactamase activity (Mine *et al.*, 1998).

β-Lactamase inhibitory activity

β-Lactamase inhibitory activity was determined according to a previously published work (Livermore and Brown, 2001; Bethel *et al.*, 2004). A 1 mM nitrocefin solution is prepared by dissolving 5.16 mg powder in 0.5 mL dimethyl sulfoxide (DMSO) then diluting with 9.5 mL 0.1 M phosphate buffer (pH 7.0). β-Lactamase activity is indicated by measuring the absorbance at 486 nm for 5 min after addition of 30 μL prepared β-lactamase to a 1-cm quartz cuvette containing 300 μL nitrocefin solution in 3 mL 0.1 M phosphate buffer (incubated at 37°C). IC_{50} values were determined by linear interpolation between the points around 50% activity of β-lactamase.

Results and discussion

Multiple alignment

According to the results obtained from multiple alignments, six amino acids Ser^{75}, Lys^{78}, Ser^{116}, Ser^{139}, Asn^{141}, and Ser^{262} of SPBP4 and five residues Ser^{454}, Asn^{456}, Thr^{584}, Gly^{585}, and Thr^{586} of SPBP2 which are near the active site pocket are found to be conserved over all species (Fig. 2).

The similarity in the three-dimensional structure of the carboxypeptidase/transpeptidase domains of PBPs is also matched by high degree of similarity in the reactive position of residues from three highly conserved motifs (Massova and Mobashery, 1998; Rhazi *et al.*, 2003; Nicola *et al.*, 2005; Kishida *et al.*, 2006; Fisher *et al.*, 2005). The first motif is the strictly conserved SXXK tetrad. The serine corresponds to the amino acid that is activated to undergo acylation in transpeptidation.

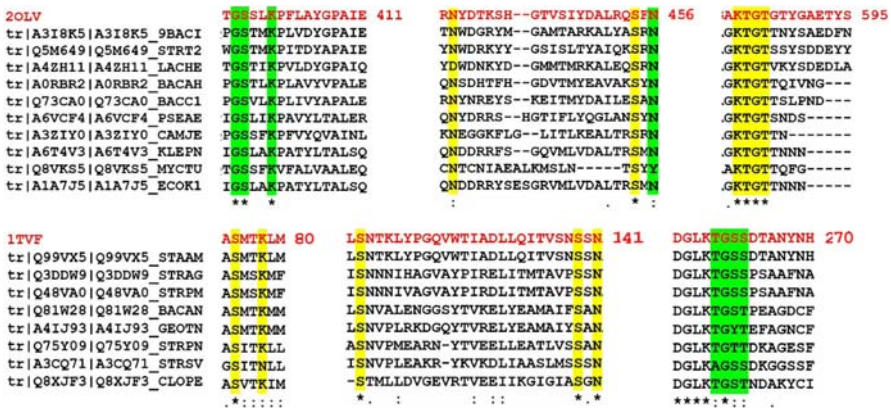

Fig. 2 ClustalX (1.81) multiple alignment of SPBP2 (*above*) and SPBP4 (*below*) distinguished by red color. The conserved amino acids in the active site pockets A and B are highlighted by yellow and green backgrounds, respectively. (Color figure online)

The lysine in this motif is the general base that activates the serine for acylation (Massova and Mobashery, 1998). The second conserved motif is the (S/Y)XN tripeptide sequence. The S/Y residue in this motif is probably required for back-donation of a proton to the nitrogen atom which makes the terminal D-Ala a better leaving group. The third conserved motif in PBPs is a KTS or KTG motif. Probably the lysine of motif III (KTG) is involved in deprotonation of the serine of motif II (SXN).

Docking analysis

On the practical level the amides **3a–j** were docked into the active sites of SPBP2 and SPBP4. SPBP4 and especially SPBP2 are the two critical penicillin binding enzymes which exist in *Staphylococcus aureus* with known crystal structure. We generated 100 docked conformers of **3a–j** using the ADT (AuoDockTools) software. The results of bacterial evaluation were in close proximity to the theoretical K_i values of docking study for those models in which amide bond oriented toward most critical residues Ser^{75} and Ser^{139} (for SPBP4) and Ser^{398} and Ser^{454} (for SPBP2) (Massova and Mobashery, 1998) (Fig. 3), similar to orientation of D-Ala-D-Ala moiety in the active site of PBPs. The results obtained from docking studies clearly demonstrated that more than 60% of docked models had nearly identical orientations as mentioned previously. From each cluster of esters one conformer that had greater similarity with the optimum conformer (lowest K_i) of benzoate analog (**3d**) was adopted as the consensus structure and was used for further analysis (Sadeghian *et al.*, 2008). The consensus bonding conformation of **3a–j** within the SPBP2 and SPBP4 active sites is illustrated in Fig. 3.

For easy analysis of docking results, we divided the space of the active site pockets into two regions: A and B (Fig. 4) as follows:

SPBP2: region A = Asn^{436}, Tyr^{437}, Gln^{453}, Ser^{454}, Phe^{455}, Ser^{569}, Lys^{583}, Thr^{584}, Gly^{585}, Thr^{586}, His^{638}, Gln^{641}, and Gln645; region B = Gly^{397}, Ser^{398}, Lys^{401}, Asn^{456}, Leu^{496}, Gly^{497}, Gly^{498}, Gly^{587}, and Thr^{588}.

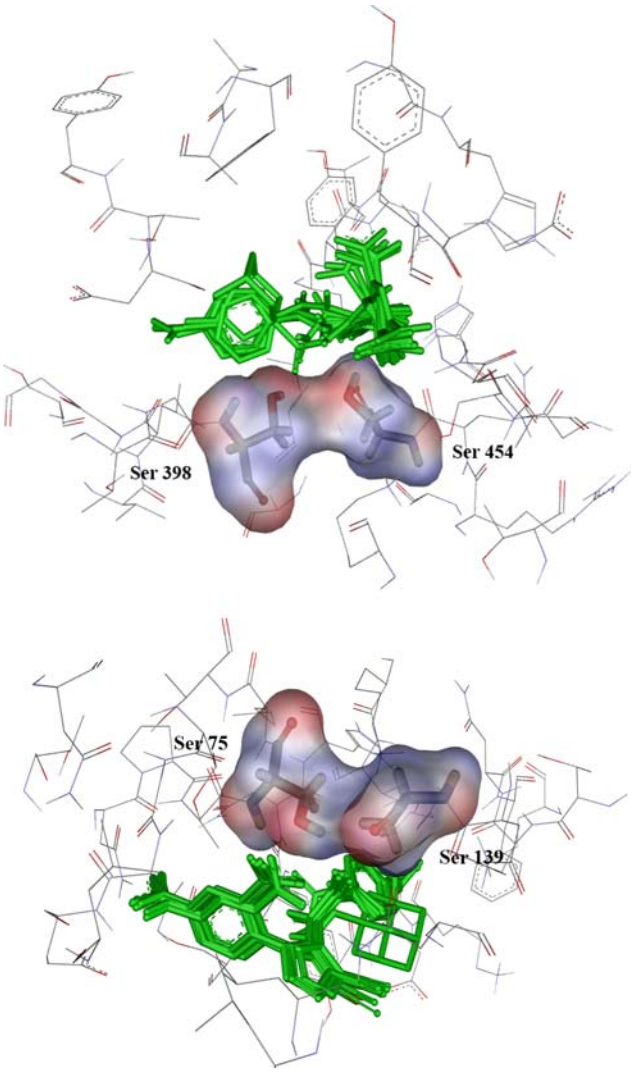

Fig. 3 Superimposition of the consensus bonding conformations of **3a–j** using green sticks in the active site of SPBP2 (*above*) and SPBP4 (*below*) within 8 Å. (Color figure online)

SPBP4: region A = Asn^{72}, Ala^{74}, Ser^{75}, Lys^{78}, Glu^{114}, Leu^{115}, Ser^{116}, Ser^{139}, Asn^{141}, Thr^{180}, Gly^{181}, Ala^{182}, Glu^{183}, Arg^{186}, Ser^{262}, Ser^{263}, and Tyr^{291}; region B = Phe^{241}, Phe^{243}, Thr^{260}, Gly^{261}, Tyr^{268}, Glu^{297}, and Arg^{300}.

It seems that, in consensus structures of docked inhibitors, 4-nitro and amide groups form hydrogen bonding with Ser^{454}, Asn^{456}, Thr^{584}, Gly^{585}, and Thr^{586} in SPBP2 (Fig. 5). In the active site pocket of SPBP4, amide group, pyrazole core, and 2,4-nitro substituents of the inhibitors have hydrogen bonding with Asn^{72}, Ser^{75}, Lys^{78}, Ser^{116}, Ser^{139}, Asn^{141}, Glu^{183}, and Ser^{262} (Fig. 5). Among the inhibitors,

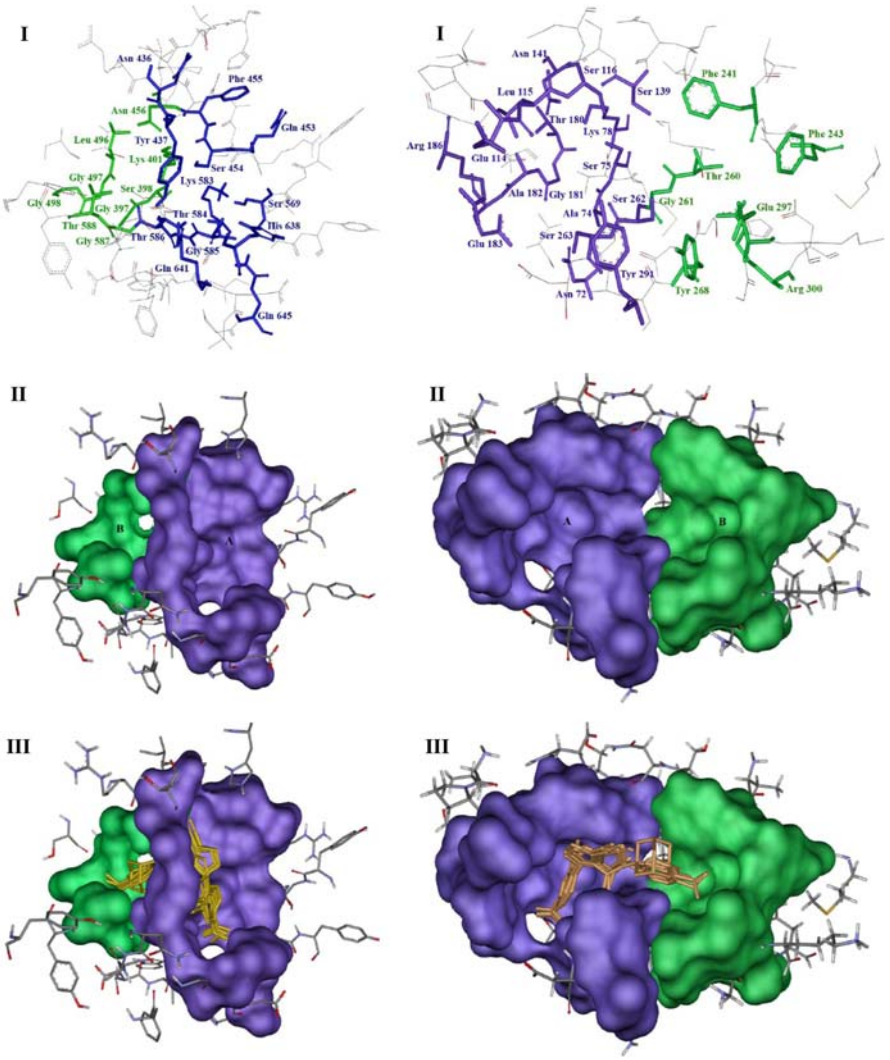

Fig. 4 X-ray presentations of SPBP2 (*left*) and SPBP4 (*right*) active site pocket in stick (I), solvent surface (II), and solvent surface docked with **3a–j** (III) views. The pockets A and B are presented in blue and green color, respectively. (Color figure online)

compounds **3i** and **3j** have hydrogen bonding with conserved Arg^{300} in the consensus docked models via their methoxy and dimethylamine groups (Fig. 5).

In SPBP2 the amide and 4-nitro groups of the proposed inhibitory model of docked molecules have hydrogen bonding with Ser^{454}, Asn^{456}, Thr^{584}, and Gly^{585} of the second and third motifs (Ser^{454}–Phe^{455}–Asn^{456} and Lys^{583}–Thr^{584}–Gly^{585}), respectively (Fig. 5). Despite the lack of hydrogen bonding between consensus structures and residues of the first motif, we witness proper orientation of hydroxyl group of Ser^{75} and Ser^{398} towards carbonyl moiety of the amides **3b–j** at distance of

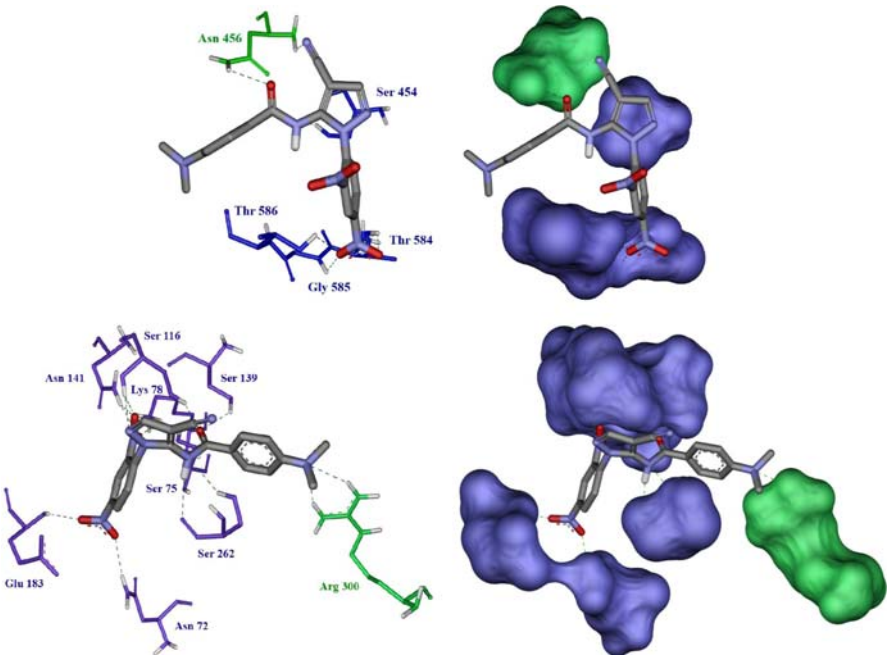

Fig. 5 Stick (*left*) and solvent surface (*right*) view of conserved amino acids of SPBP2 (*above*) and SPBP4 (*below*) which have hydrogen bonding interactions with compound **3j**. The amino acids of pocket A and B are presented in blue and green color, respectively. (Color figure online)

3–3.5 Å for intermolecular interaction (Fig. 6). As seen in Fig. 5, the first and second motifs of SPBP4 (Ser^{75}–Met^{76}–Thr^{77}–Lys^{78} and Ser^{139}–Ser^{140}–Asn^{141}) have hydrogen bonding with amide and 2-nitro groups of the proposed inhibitory models of docked molecules. In both docked models of SPBP2 and SPBP4, Ser^{454} and Ser^{262} acts as proton donors for hydrogen bonding with NH of the inhibitors (Fig. 6).

The K_i values of proposed model of compounds **3d–j** obtained from docking with SPBP2 and SPBP4 had good relationships with obtained MIC values (Fig. 7). Such conformity between MIC and K_i values of these compounds can be accounted for by the tendency of substituted benzoate moiety to fill the empty space of pocket B in SPBP2 and SPBP4. Among the synthetic inhibitors, compounds **3g**, **i**, and **j** showed the best inhibitory effects against MRSA and MSSA (MIC **3g** = 27.4 μM; **3i** = 15.3 μM; **3j** = 3.8 μM for both strains) (Fig. 1). These results are comparable with MIC values of cephalexin (72 and 4.6 μM) and cloxacillin (94 and 13.7 μM). The K_i values of compounds **3g**, **i**, and **j** obtained from docking with SPBP2 and SPBP4 are the smallest values among the other compounds (in SPBP2: K_i (**3g**) = 3.10e-7, K_i (**3i**) = 5.03e-7, and K_i (**3j**) = 1.85e-7 and in SPBP4: K_i (**3g**) = 7.39e-9, K_i (**3i**) = 5.43e-9, and K_i (**3j**) = 2.27e-9).

It is notable that these compounds showed β-lactamase inhibitory activity (Table 2). This property was tested for compounds **3f–j** by using the nitrocefin test (Bethel *et al.*, 2004). The results of Table 2 show that these compounds can inhibit

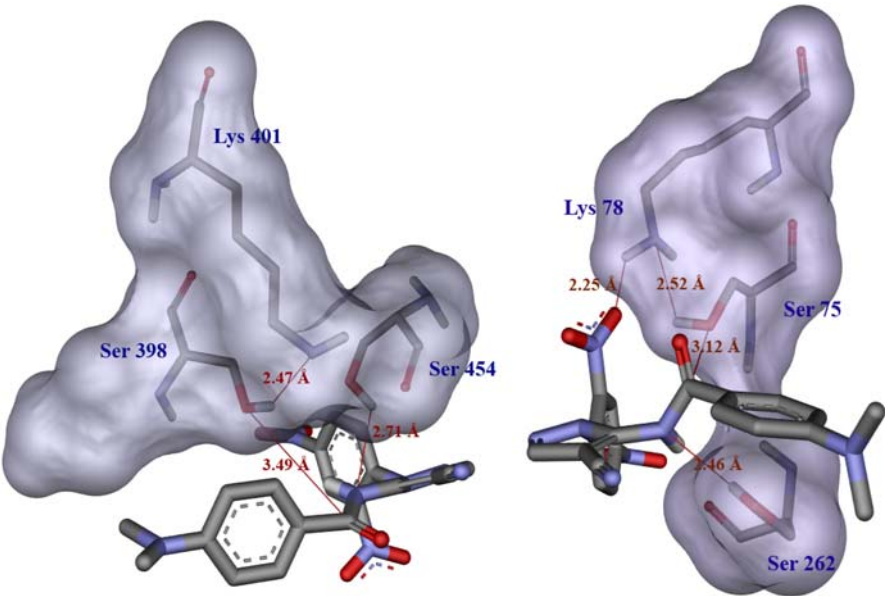

Fig. 6 Presentation of intermolecular interaction of consensus bonding conformation of compound 3j with SXXK motifs in SPBP2 (*left*) and SPBP4 (*right*). Carbon, nitrogen, oxygen, and hydrogen atoms are presented in gray, blue, red, and white colors, respectively. (Color figure online)

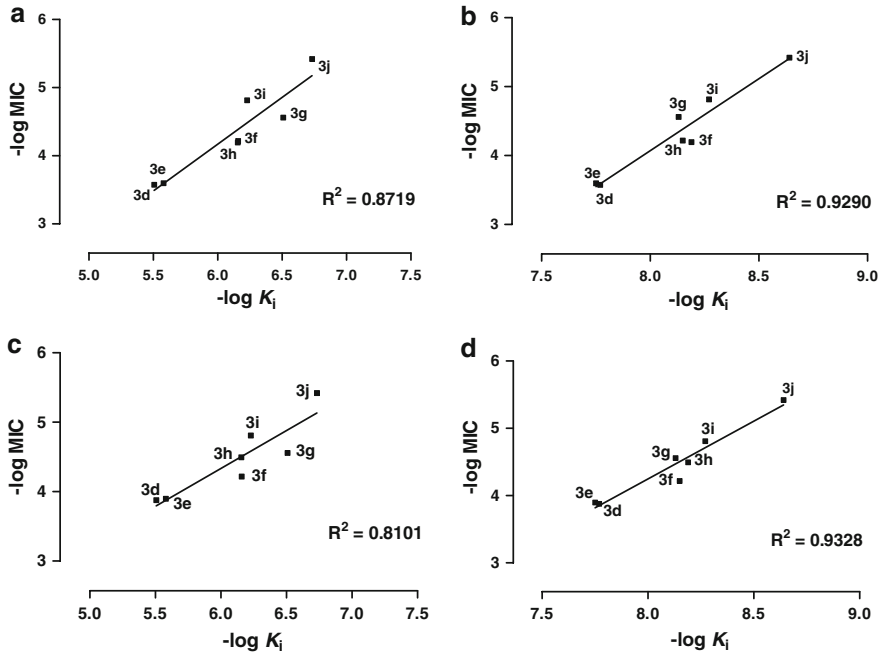

Fig. 7 Diagrams of −log MIC versus −log K_i of consensus bonding conformation of compounds **3d–j** for SPBP2 (**a** and **c**) and SPBP4 (**b** and **d**). Diagrams **a** and **b** relate to MRSA and diagrams **c** and **d** related to MSSA

Table 2 β-Lactamase inhibitory activity of compounds **3f–j**

Compound	**3f**	**3g**	**3h**	**3i**	**3j**
IC_{50}	84 ± 6	49 ± 5	94 ± 5	35 ± 4	43 ± 4

The IC_{50} values are given as ± standard deviation (SD)

β-lactamase activity. Considering the SAR results and also the similarity between the active site of DD-peptidases and β-lactamases (Massova and Mobashery, 1998; Rhazi *et al.*, 2003; Nicola *et al.*, 2005; Kishida *et al.*, 2006; Fisher *et al.*, 2005), these results can provide good proof for the affinity of these compounds towards PBPs.

Conclusions

We carried out SAR comparative studies of 5-amino-1-(2,4-dinitrophenyl)-1*H*-4-pyrazolecarbonitrile carboxylates as *S. aureus* growth inhibitors and proposed the theory of PBP inhibitory mechanism for these amides. We have also shown the important role of amide functionality in the inhibitory activities of compounds **3a–j**, which paves the way for further investigation of larger and more polarizable substituents at *para* position of the benzamide moiety to evaluate their effect on Gram-positive bacteria and their PBPs activities.

Acknowledgements We would like to express our sincere gratitude to Mr. Mahmood Ramezanpour (Laboratory of Microbiology, Ghaem Hospital, Mashhad University of Medical Sciences, Mashhad, Iran) for financial support of this work.

References

Adediran SA, Cabaret D, Flavell RR, Sammons A, Wakselman M, Pratt RF (2006) Synthesis and beta-lactamase reactivity of alpha-substituted phenaceturates. Bioorg Med Chem 14:7023–7033. doi:10.1016/j.bmc.2006.06.023

Ahn YM, Pratt RF (2004) Kinetic and structural consequences of the leaving group in substrates of a class C beta-lactamase. Bioorg Med Chem 12:1537–1542. doi:10.1016/j.bmc.2003.12.042

Ammar YA, Al-Sehemi AG, El-Gaby MSA, El-Sharief AMS, Zahran MA, El-Said UH (2004) Some reactions with ketene dithioacetals. Part III: Novel synthesis of pyrimidine, pyrazole and pyrazolo[3,4-d]pyrimidine derivatives as antimicrobial agents. Afinidad 61:261–265

Bakavoli M, Nikpour M, Rahimizadeh M, Saberi MR, Sadeghian H (2007) Design and synthesis of pyrimido[4,5-b][1,4]benzothiazine derivatives, as potent 15-lipoxygenase inhibitors. Bioorg Med Chem 15:2120–2126. doi:10.1016/j.bmc.2006.12.022

Bakavoli M, Sadeghian H, Tabatabaei Z, Rezaei E, Rahimizadeh M, Nikpour M (2008) SAR comparative studies on pyrimido[4,5-b][1,4] benzothiazine derivatives as 15-lipoxygenase inhibitors, using ab initio calculations. J Mol Model 14:471–478. doi:10.1007/s00894-008-0298-8

Bethel CR, Hujer AM, Helfand MS, Bonomo RA (2004) Exploring the effectiveness of tazobactam against ceftazidime resistant Escherichia coli: insights from the comparison between susceptibility testing and beta-lactamase inhibition. FEMS Microbiol Lett 234:99–103

Bugg TD, Walsh CT (1992) Intracellular steps of bacterial cell wall peptidoglycan biosynthesis: enzymology, antibiotics, and antibiotic resistance. Nat Prod Rep 9:199–215. doi:10.1039/np9920900199

Cookson B (2005) Clinical significance of emergence of bacterial antimicrobial resistance in the hospital environment. J Appl Microbiol 99:989–996. doi:10.1111/j.1365-2672.2005.02693.x

Dym O, Xenarios I, Ke H, Colicelli J (2002) Molecular docking of competitive phosphodiesterase inhibitors. Mol Pharmacol 61:20–25. doi:10.1124/mol.61.1.20

Ergenc N, Durgun B, Otuk G (1992) Studies on azopyrazole derivatives. 9. Synthesis and antibacterial evaluation of novel phenylhydrazines and their substituted 4-arylazopyrazole derivatives. Pharmazie 47:495–498

Finegold SM, Garrod L (1995) Bailey and Scott's diagnostic microbiology, Chap. 13, 8th edn. C.V. Mosby Co., Toronto, pp 171–193

Fisher JF, Meroueh SO, Mobashery S (2005) Bacterial resistance to β-lactam antibiotics: compelling opportunism, compelling opportunity. Chem Rev 105:395–424. doi:10.1021/cr030102i

Free SM, Wilson JW (1964) A mathematical contribution to structure–activity studies. J Med Chem 7:395–399. doi:10.1021/jm00334a001

Ghafourian T, Barzegar-Jalali M (2002) Theoretical modeling of oral absorption of barbiturates. Farmaco 57:565–567. doi:10.1016/S0014-827X(02)01249-1

Hansch C (2003) QSAR and the role of luck in research. Farmaco 58:621–623. doi:10.1016/S0014-827X(03)00175-7

Kishida H, Unzai S, Roper DI, Lloyd A, Park SY, Tame JRH (2006) Crystal structure of penicillin binding protein 4 (dacB) from *Escherichia coli*, both in the native form and covalently linked to various antibiotics. Biochemistry 45:783–792. doi:10.1021/bi051533t

Kreutzberger A, Burgwitz K (1980) Antibacterial agents. IV. Nitro substitution in the 5-amino-4-cyanopyrazole series. J Heterocycl Chem 17:265–266

Li Z, Francisco GD, Hu W, Labthavikul P, Petersen PJ, Severin AY, Singh G, Yang Y, Rasmussen BA, Lin Y, Skotnicki JS, Mansour TS (2003) 2-Phenyl-5,6-dihydro-2*H*-thieno[3,2-c]pyrazol-3-ol derivatives as new inhibitors of bacterial cell wall biosynthesis. Bioorg Med Chem Lett 13:2591–2594. doi:10.1016/S0960-894X(03)00471-2

Livermore DM, Brown DF (2001) Detection of beta-lactamase-mediated resistance. Antimicrob Agents Chemother 48:59–64

Massova I, Mobashery S (1998) Kinship and diversification of bacterial penicillin-binding proteins and β-lactamases. Antimicrob Agents Chemother 42:1–17

Mine Y, Kamimura T, Wabe Y, Tawara S, Matsumoto Y, Shibayama F (1988) In vitro antibacterial activity of FK482, a new orally active cephalosporin. J Antibiotics 12:1873–1887

Morris GM, Goodsell DS, Halliday RS, Huey R, Hart WE, Belew RK, Olson AJ (1998) Automated docking using a Lamarckian genetic algorithm and an empirical bonding free energy function. J Comput Chem 19:1639–1662. doi:10.1002/(SICI)1096-987X(19981115)19:14<1639::AID-JCC10>3.0.CO;2-B

Nicola G, Peddi S, Stefanova M, Nicholas RA, Gutheil WG, Davies C (2005) Crystal structure of *Escherichia coli* penicillin-binding protein 5 bound to a tripeptide boronic acid inhibitor: a role for Ser-110 in deacylation. Biochemistry 44:8207–8217. doi:10.1021/bi0473004

Nieto MJ, Alovero FL, Manzo RH, Mazzieri MR (2005) Benzenesulfonamide analogs of fluoroquinolones. Antibacterial activity and QSAR studies. Eur J Med Chem 40:361–369. doi:10.1016/j.ejmech.2004.11.008

Patel HV, Fernandes PS, Vyas K (1990) A novel synthesis of a few substituted sym-triazolo[3,4-b[1,3,4]thiadiazoles and evaluation of their antibacterial activity. Indian J Chem B 29:135–141

Phillips L, Willians JD, Wise R (1978) Laboratory methods In antimicrobial chemotherapy. Churchill Livingston, Edinburgh, p 3

Pordel M (2004) Synthesis of new derivatives of Aminopyrazolocarbonitril. M.Sc. thesis, Ferdowsi University of Mashhad, Mashhad, Iran

Pratt RF, Govardhan CP (1984) beta-Lactamase-catalyzed hydrolysis of acyclic depsipeptides and acyl transfer to specific amino acid acceptors. Proc Natl Acad Sci USA 81:1302–1306. doi:10.1073/pnas.81.5.1302

Prescott LM, Harley JP, Klein DA (2002) Microbiology, Chap. 3, 5th edn. McGraw-Hill, New York, pp 57–60

Python MFS (1999) A programming language for software integration and development. J Mol Graph Model 17:57–61

Rhazi N, Charlier P, Dehareng D, Engher D, Vermeire M, Fre're J, Nguyen-Diste'che M, Fonze E (2003) Catalytic mechanism of the Streptomyces K15 DD-transpeptidase/penicillin-binding protein probed

by site-directed mutagenesis and structural analysis. Biochemistry 42:2895–2906. doi:10.1021/bi027256x

Sadeghian A, Seyedi SM, Sadeghian H, Hazrathoseyni A, Sadeghian M (2007) Synthesis, biological evaluation and QSAR studies of some new thioether-ester crown ethers. J Sulfur Chem 28:597–605. doi:10.1080/17415990701670718

Sadeghian H, Seyedi SM, Saberi MR, Arghiani Z, Riazi M (2008) Design and synthesis of eugenol derivatives as potent 15-lipoxygenase inhibitors. Bioorg Med Chem 16:890–901. doi:10.1016/j.bmc.2007.10.016

Schmidt P, Eichenberger K, Druey J (1958) Heilmittelchemische Studien in der heterocyclischen Reihe. 22. Mitteilung. Pyrazolo-pyrimidine II Pyrazolo[3,4-d]pyrimidine mit Koffein-ähnlicher Struktur und Wirkung. Helv Chim Acta 41:1052–1060. doi:10.1002/hlca.19580410418

Sippl W (2000) Receptor-based 3D-QSAR analysis of estrogen receptor ligands—merging the accuracy of receptor-based alignments with the computational efficiency of ligand-based methods. J Comput Aided Mol Des 14:559–572. doi:10.1023/A:1008115913787

Thompson JD, Gibson TJ, Plewniak F, Jeanmougin F, Higgins DG (1997) The ClustalX windows interface: flexible strategies for multiple sequence alignment aided by quality analysis tools. Nucleic Acids Res 24:4876–4882. doi:10.1093/nar/25.24.4876

Villani FJ, King MS (1963) 3-Benzoylpyridine. Org Syn Coll 4:88–89